Recognition of Human Body Posture from a Cloud of 3D Data Points using Wavelet Transform Coefficients

Naoufel Werghi Yijun Xiao
Department of Computing Sciences
University of Glasgow
Glasgow G12 8QQ
naoufelw@dcs.gla.ac.uk

Abstract

This paper addresses the problem of recognizing a human body posture from a cloud of 3D points acquired by a Human body scanner. Motivated by finding a representation that embodies a high discrimination power between posture classes, a new type of features is suggested, namely, the wavelet transform coefficients (WTC) of the 3D data points distribution projected on the space of the spherical harmonics. A Feature selection technique is developed to find the features with high discriminatory power. Integrated within a Bayesian classification framework and compared with other standard features, the WTC showed great capabilities in discriminating between close postures. The qualities of the WTC features were also reflected on the experiment results carried out with artificially generated postures, where the WTC got the best classification rate. To the best of our knowledge, this work appears to be the first to treat the posture recognition in the three-dimensional case and to suggest WTC as features for 3D shape.

1. Recognizing a 3D Human Body posture: Why ?

The recent years have seen the emergence of human body scanners capable of capturing the whole shape as well as the appearance of the human body (HB). New perspectives were opened for the exploitation of this technology in various sectors. In entertainment , scans of real persons can be mapped to generic models and then integrated in video games, TV or cinema production [1]. In clothing industry, human body scans can substitute the real person for extracting measurements [2, 3, 4]. Data bases of HB scans can be useful for medical and anthropological surveys [5]. Many of these applications need decomposing the body shape into surfaces corresponding to the different parts of the human body, namely the head, the upper arms, the lower arms, the upper legs, the bottom legs and the torso.

There have been some attempts to segment automatically human body shape [2, 3, 4] however these works treated the particular case of a standard posture (Figure 1.(a)). Their techniques were restrictive and cannot handle arbitrary postures. Our believe is that tackling the segmentation of human body shape without any prior knowledge of the body posture is a very difficult problem. Retrieving first the HB posture will make the segmentation problem more approachable by providing information about the relative locations of the human body parts. This information is also valuable for model conformation problems where we want to fit a generic model to 3D HB scan. The posture knowledge can be used in that case to find an initial rough confor-

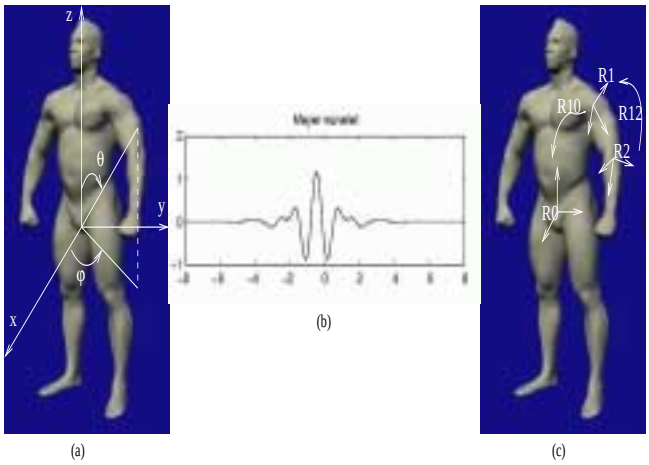

Figure 1. (a): the standard posture of a human body in a reference frame (x, y, z) attached to the scanner. A rotation of the whole HB is constrained to be around the z axis, affecting only the angle ϕ. (b):Meyer wavelet function. (c) The body parts orientation are hierarchy defined . The rotation R_{12} between $R1$ and $R2$ defines the orientation of the lower left arm with respect to the upper left arm and this one's orientation is defined by the rotation R_{10} between R_1 and R_0.

Proceedings of the Fifth IEEE International Conference on Automatic Face and Gesture Recognition (FGR'02)
0-7695-1602-5/02 $17.00 © 2002 IEEE

mation that can be refined afterwards. This task used to be performed manually, as for instance in [1].

Therefore the aim of this work is to recognize a HB postures from 3D HB scans. We propose to achieve this objective within a model-based approach where the problem is stated as follows: Given a set of posture models and given a query posture, find which posture model corresponds to the query posture. The paradigm followed to solve this problem is built upon three elements: representation, feature extraction and classification or decision.

The rest of the paper is organized as follows, Section 2 emphasizes the important role of the representation and describes the WTC features. Section 3 presents a Bayesian approach for classifying the postures. It also describes the feature selection scheme based on which the best features, in terms of discrimination power are chosen. Section 4 exposes the experimental side of this work, it describes the generation of the model postures and illustrates, within a comparative study, the advantages of the features having a high discrimination power, and show as well their impact on the classification. The paper is concluded by discussing the results, potential improvements and future work.

2. Representation

In shape recognition techniques, objects are represented by numerical features in order to remove the redundancy of the data and to reduce its dimension. The features are often grouped into vectors. The data we deal with, is a scattered 3D points representing the human body surface shape. Most of the HB scanners provide a complete data that covers the whole surface of the body. This is encouraging to investigate what global features can offer for 3D shape identification. The moment features have been extensively used in image analysis and description. The attention was mainly oriented towards moments that are invariant with respect to translation, rotation and scale. Such moments were first proposed by Hu [6]. Then a variety of moments were developed later, particularly the orthogonal moments [7] , such Legendre moments, Fourier-Mellin moments, Zernike moments and pseudo-Zernike moments. The orthogonal moments have shown to be less redundant,less sensitive to noise and more informative than geometrical moments. A nice survey and comparison of 2D moments can be found in [8] where Zernike moments have shown to have the best overall performance.

Less work has been done in exploiting moments in the case of three-dimensional data However. One of the reasons, is that most of the 3D Imaging devices so far do not provide complete data in terms of surface covering. Condition which is necessary for any global feature based analysis. Nnevertheless, there have been some attempts to define frameworks for 3D moments construction. Sadjadi *et al* [9] pioneered the development of 3D Geometric moment invariants. Their framework built a family of three invariant moments with a degree up to the second-order. Using the notion of complex moments Lo *et al* [10] constructed a family of twelve invariant moments with orders up to the third degree. However, in these last works, moments were used mainly to estimate 3D transformations and their performances were not evaluated for classification tasks. Also, these moments are not derived from a family of orthogonal functions, they are therefore subject to correlation.

2.1. The Wavelet-basedrepresentation

The Wavelet concept was introduced by Morlet [11] as time-scale analysis tool for non-stationary signals. It was further developed by many authors [12, 13, 14] and rapidly found applications in many areas. A wavelet function is a function that is well localized in the space and the frequency domain. From a mother function $g(r)$ a family of wavelet functions $g_{a,b}(r) = \frac{1}{a} g(\frac{r-b}{a}), a > 0$ is derived. This family is obtained by shifting the wavelet mother by b (the shifting parameter) and by dilating (stretching) it with a (the scaling parameter). The wavelet transform at the scale a and the shift b is: $\int_{-\infty}^{\infty} f(r) g_{a,b}(r) dr$. The wavelet transform embodies information about the regularity and the spectrum of the frequency around the position b at the scale a. From this perspective it is seen as a local operator, however by varying the parameter b along the domain of the function $f(r)$ we can get a global description of the function. Let consider $f(r, \theta, \phi)$ a 3D binary representation of the cloud of 3D data points in the spherical coordinates. In its discrete form, $f(r, \theta, \phi)$ can be seen as spherical voxel representation. We would like to analyze and identify the distribution of the cloud of points over the space (r, θ, ϕ). Consider a sphere of radius r, the points distribution at the sphere surface can be described by the spherical harmonics via the transformation: $F_{mn}(r) = \int_0^{2\pi} \int_0^{\pi} f(r, \theta, \phi) U_{m,n}(\theta, \phi) r^2 sin\theta d\theta d\phi, \quad 0 \leq m \leq n$ where $U_{m,n}$ are the spherical harmonics of order m and n defined on the unit sphere. they form an orthogonal family [15], expressed by $U_{m,n} = e^{jm\phi} V_n(\theta)$ where $V_n(\theta)$ is a polynomial function of order n in $cos\theta$ and $sin\theta$. $F_{mn}(r)$ define therefore a sort of moments that describe the distribution of points on the spherical surface of radius r. We considered the first four spherical harmonic functions namely, $U_{0,0} = 1,\ U_{0,1} = cos\theta,\ U_{1,1} = e^{j\phi} sin\theta,\ U_{1,2} = -3e^{j\phi} sin\theta cos\theta.$

Now what remains is to describe the variation of these moments in function of r to obtain a 3D description of the posture. This description should infers a multi-scale aspect since the variation in the posture distributions manifests at different scales. This can be seen, if we examine for example, the pairs of postures $(2, 18)$ and $(6, 8)$ in Figure 2. For the first pair, difference in data point distribution covers more than the half of the posture space, whereas it is lim-

Feature	$C^{0,1}_{1,1}$	$C^{1,1}_{1,2}$	$C^{0,1}_{1,2}$	$C^{0,1}_{3,15}$	$C^{0,1}_{3,13}$	$C^{0,1}_{2,6}$	$C^{0,0}_{1,2}$	$C^{0,0}_{2,7}$	$C^{1,1}_{0,2}$	$C^{1,1}_{2,3}$	$C^{0,0}_{2,2}$	$C^{0,1}_{2,7}$
J x 10e6	8.880	6.673	0.864	0.548	0.212	0.163	0.157	0.154	0.122	0.116	0.111	0.0996

(a)

Feature	$C^{0,0}_{3,7}$	$C^{0,1}_{3,7}$	$C^{2,1}_{3,9}$	$C^{1,1}_{3,11}$	$C^{1,1}_{3,10}$	$C^{0,1}_{3,11}$	$C^{0,0}_{3,10}$	$C^{0,0}_{3,12}$	$C^{1,1}_{3,9}$	$C^{1,1}_{3,12}$	$C^{2,1}_{3,9}$	$C^{1,1}_{3,16}$
J x 10e3	3.155	3.309	3.941	4.020	4.109	4.379	4.382	4.501	4.565	4.584	4.629	4.719

(b)

Table 1. (a) The first 12 best features ranked in descending order. (b) the worst 12 features ranked in ascending order

ited to the volume around the right arm for the second pair. Being a multi-scale operator, the wavelet transform satisfies this requirement. We define therefore the WTC of the moment functions $F_{mn}(r)$ as $C^{mn}_{ab} = \int_0^\infty F_{mn}(r)\psi_{a,b}(r)dr$ The mother wavelet function we utilized is Meyer's wavelet [14] (Figure1.(b)), it is highly regular (has an infinite number of vanishing moments), has a compact support and generates an orthogonal basis of function ψ_{ab}. This allows to form an orthogonal family $F_{mn}(r)\psi_{a,b}(r)$. The coefficients C^{mn}_{ab} are then derived from a family of orthogonal functions. They can be seen as a particular type of orthogonal 3D moments. We precise also that the feature we consider here is the module of the wavelet transform coefficient (WTC) defined by $\sqrt{< C^{mn}_{ab}, C^{*mn}_{ab} >}$.

The invariance of the WTC with respect to translation and scale is obtained by preprocessing the data in the Cartesian space before passing to the spherical space. From the cloud of 3D data points a Cartesian voxel grid if formed. Then the origin of the voxel grid is shifted to the centre of mass of the data points. The scale invariance is obtained by affecting the 3D points' coordinates so that the data volume defined by the moment $m_{000} = \sum_x \sum_y \sum_z f(x,y,z)$ is equal to V_0, where V_0 is a predetermined value. The rotation of the whole HB within the scanner has only one degree of freedom that affects only ϕ. It can be shown easily that$\|C^{mn}_{ab}\|$ is invariant with respect to that rotation. The negative side is that pairs of symmetric postures have very close feature values. Such pairs have been associated to the same class and the ambiguity can be removed after the classification using simple geometric procedures.

A dyadic discretization is adopted for a and b, by choosing $a = (Scale)2^{-p}$, $p = 0,1,2,3$ and $b = qa/2$, $q = 0,1,...,2^{p+1}$, where $Scale$ is the radius of the sphere confining the data points. The scaling parameter a takes the values $Scale, Scale/2, Scale/4, Scale/8$. Values smaller than $Scale/8$ do not allow to extract significant information. The shifting parameter b is varied proportionally to the scale parameter within the range $[0, Scale]$. The number of (p,q) pairs is then equal to 34, which combined with 4 pairs (m,n) result in 136 WTC features C^{mn}_{pq} .

3. The classification problem

The classification problem is stated as follows: Given a set of posture classes $C_1, ..C_N$ and given a query posture Q, to which class the posture Q belongs. The query posture is represented by an observation feature vector of dimension d, $X = [x_1, x_2, .., X_d]$. For each class C_i, let consider the discriminative functions $d_i(X)$. The observed feature vector is associated to the class C_i if $d_i(X) > d_j(X)$ for all $j \neq i$. The optimal discriminative function in the sense of Bayes is the one defined as the *aposteriori* conditional probability function $P(C_i|X)$, expressed according to Bayes' rule by $P(C_i|X) = \frac{P(X|C_i)P(C_i)}{P(X)}$. Since any monotonically increasing function of$P(C_i|X)$ leads to identical classification result the following function is rather considered: $d_i(X) = ln(P(X|C_i)P(C_i))$,defined as the logarithm of the product of the likelihood of the class C_i with respect to X and the $apriori$ probability function $P(C_i)$. Assuming that the $P(X|C_i)$ is a normal density $\mathcal{N}(\mu_I, \Sigma_i)$ defined by $p(X|C_i) = \frac{1}{2\pi|\Sigma_i|^{1/2}} exp[-\frac{1}{2}(X-\mu_i)^T\Sigma_i^{-1}(X-\mu_i)]$, and the the different classes have equal $apriori$ probability, the expression of the discriminative function can be brought to $d_i(X) = -\frac{1}{2}(X-\mu_i)^T\Sigma_i^{-1}(X-\mu_i) - \frac{1}{2}ln|\Sigma_i|$. The statistics (μ_i, Σ_i) of class C_i are obtained from training process based using the standard EM technique [16]

3.1. Selection of discriminative features

Naturally the set of wavelet coefficients has redundancy since not all the coefficients contribute effectively in the classification. There is a need to select the most useful features that have a high discriminative power. The discriminative power is characterized by the interclass distance defined as metric for measuring the separation between two classes. A selection criterion based on that metric is therefore utilized in the search for the optimal set of features. Extracting the optimal set of features was subject of intensive work in the literature [17]. There are mainly tow categories of techniques the first operates on feature vectors, the second treats each feature individually. We adopted a technique belonging to the second one, it is sub-optimal but quite efficient. The selection algorithm is as follows: Given a set of features $\{x_1, x_2, .., x_d\}$ and given a selection criterion J:

1) Compute the selection criterion value $J(k)$ for each feature x_k , 2) rank the features in descending order with

respect to J, 3) select the first best features and construct with them the feature vector.

3.1.1 The interclass distance

The choice of the selection criterion is quite tight to the classification method in the sense that the interclass distance should be defined in the same framework that of the classification scheme. The interclass distance between two classes C_i and C_j having the conditional probability density functions $P(x_k, C_i) = \mathcal{N}(\mu_i^k, \sigma_i^k)$ and $P(x_k, C_j) = N(\mu_j^k, \sigma_j^k)$ with respect to the feature x_k can be evaluated by the following probabilistic separation: $d_{ij}^k = \frac{1}{2}(\frac{\sigma_j^k}{\sigma_i^k} + \frac{\sigma_i^k}{\sigma_j^k} - 2) + \frac{1}{2}(\mu_i^k - \mu_j^k)^2(\frac{1}{(\sigma_i^k)^2} + \frac{1}{(\sigma_j^k)^2})$.

This expression indicates that the larger the ratio of the means difference and the variances sum, the wider is the distance separating the two classes. The criterion that evaluates the discriminative power of the feature x_k is then the sum of the pairwise interclass distance: $J(k) = \sum_{i=1}^{d} \sum_{j=i+1}^{d} d_{ij}^k$. The larger the value of J, the better the feature x_k can discriminate between the classes.

This criterion is then used to rank the set of the 136 features $C_{p,q}^{m,n}$. Table 2.1 shows the first 12 best features and the 12 worst features. Although it not straightforward to interpret these tables , some remarks can be noticed yet. For example most the good features in Table 1.(a) have a relatively large scale parameter,for instance the 2 first ones, namely, $C_{1,1}^{0,1}$ and $C_{1,1}^{1,2}$ have a scale parameter equal to $a = Scale/2$. The scale parameter of $C_{3,15}^{0,1}$ and $C_{3,13}^{0,1}$ is equal to $Scale/16$ however the shift parameters are high (15 Scale/16 and 13 Scale/16), so these features operate on the periphery of 3D data points volume, area which is the most sensitive to posture changes caused by the arms' gesture in our models. For the worst features, in Table 1.(b), it can be noticed that they share all the lowest scale parameter value, namely (Scale/16). This reflects the poorness of information in the low scale features.

4. Experiments

A set of experiments were carried out to assess the performance of the WTC features in terms of power discrimination and classification rate. This was done within a comparative study that evaluated the performances of the WTC features against the geometric moments developed by Lo *et al* [10] and the 3D Zernike moments [18]

4.1. Generation of the posture models

The posters are generated from 3D Human body scan obtained from Cyberware cite in the Web [19] . This scan was segmented manually using a software package AMES

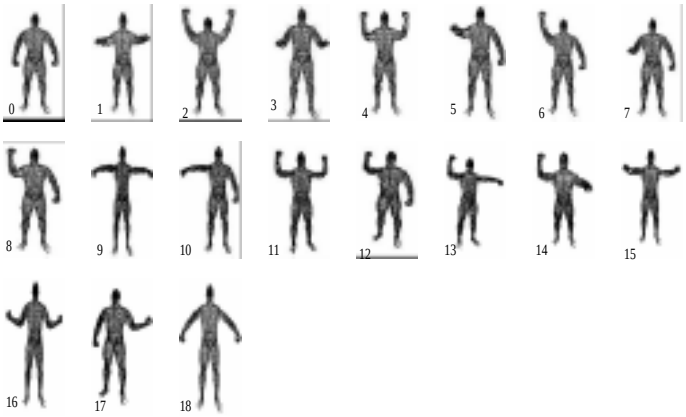

Figure 2. The posture models

[20] developed in our Lab. The data was decomposed into groups corresponding to the different parts of the HB namely, two lower arms, two upper arms, two legs and the torso (including the head). These parts were associated to a hierarchical jointed structure model that satisfies the kinematics constraints of the human body. This model was created using the Software AHBM [21], developed also in our lab, and offering an interactive animation of the human body. In this model, a body segment location (position and orientation) is defined relatively to the upper segment in the body hierarchy, for instance the position and orientation of the right lower arm are defined with respect to a reference attached to the right upper arm (Figure 1.(c)) . The relative orientations of the human body segments constitute the parameters of a given posture. By varying these parameters a variety of postures having a reasonable human appearance can be obtained. The statistic characteristic of each posture models are determined as follows, for each posture, 30 training data sets are generated, perturbing at each generation the posture parameters with a Gaussian noise and randomly rotating the full data in a direction that affects the ϕ coordinate. The mean and the variance of the model vectors are computed upon the 30 feature vectors associated to the training sets. This methods leads to a more realistic statistics than corrupting each 3D data point individually, since in real conditions the deviations of the posture parameters with respect to the real ones are caused mainly by the body movements rather than the HB scanner noise. Figure 2 shows the different posture models labelled from 0 to 18.

4.2. Comparison of the discriminative power

The discriminative power for each of the geometric moments, Zernike moments and the WTC is assessed by examining how well the best features of each category can

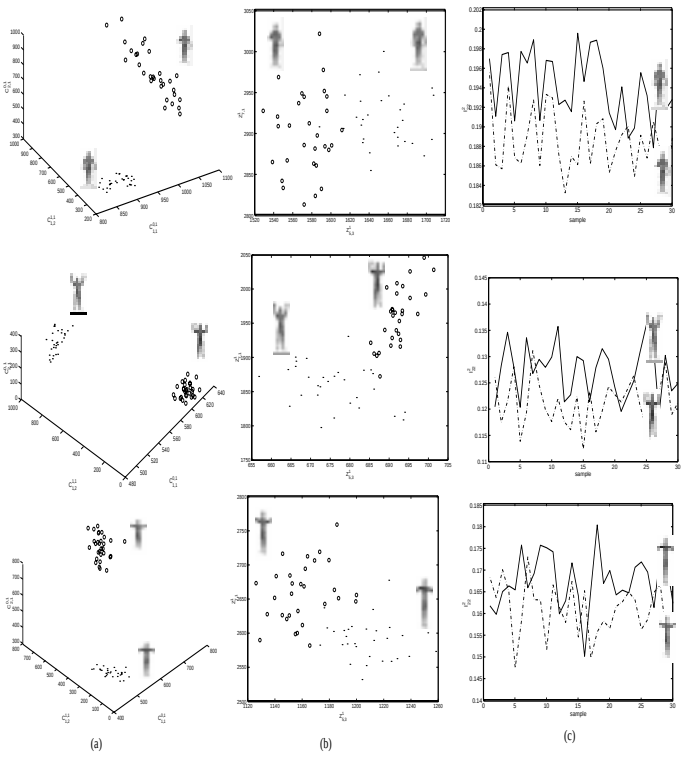

Figure 3. Distribution of best features for the three pairs of close postures. (a) variation of the three best WTC features $C^{0,1}_{1,1}$, $C^{1,1}_{1,2}$ and $C^{0,1}_{2,1}$. (b) variation of the two best Zernike moments $Z_{5,3}$ and $Z_{7,1}$. (c) variation of the geometric moment I^2_{22}.

discriminate between close postures. The best features for the geometric moments and Zernike moments were selected using the same scheme than for the WTC. From the posture models we selected pairs of postures which are close, namely $(posture_0, posture_7)$, $(posture_2, posture_{11})$ and $(posture_2, posture_{9_15})$. Then for the 30 training samples of each posture in the pair, we plot the values of their corresponding best features. The distributions related to each posture could then be visually compared.

Figure 3.a shows that the first three WTC features, namely, $C^{0,1}_{1,1}$, $C^{1,1}_{1,2}$ and $C^{0,1}_{2,1}$ are clearly well separated for the three pairs. The separation of the two best Zernike moments $Z^1_{5,3}$ and $Z^1_{7,1}$ plotted in a same figure for each pair (Figure 3.b) is less clear although their distributions can be distinguished. A more mixed close distributions are noticed for the two other best Zernike moments.

The distributions of the best geometric moment I^2_{22} in Figure 3.c, look mixed, particularly for the two last pairs. The distributions of the two other best geometric moments have similar behaviour.

The figure revels that the WTC features are more capable to distinguish between close postures than Zernike moments whereas the geometric moments are far less competitive. It is worth to mention also that the three best WTC features were not selected specifically to discriminate between these particular close postures, since the selection process involved all the postures and consequently they might not be the optimal features to discriminate between these particular ones, however these features still do separate them quite reasonably.

4.3. Comparison of the Classification rate

In these experiments, a set of query of test postures is matched with the posture models, the performances of the WTC features, Zernike moments and geometrical moments are assessed by evaluating the rate of successful classifications. Query postures were obtained with AHBM software, in the same way than the posture models, that is a 30 randomly perturbed and rotated version for each artificially generated posture.

The first test involved the three categories of features. The aim is to have a rough comparison between them rather than assessing their individual performances. This test was carried out with the best four features of each category. The query postures are composed of 20×19 samples. The results are illustrated in Figure 4.(a) the WTC has best rating followed by Zernike moments whereas the geometric moments have the lower rating . The other assessed aspect in the experiments concerns how the classification rate evolves in function of the number of features. This gives an idea about the optimality of the selected set of features. In this experiment, only the WTC and the Zernike moments were assessed, as we decided not to carry with geometric moments, based on the results of the previous experiment. This experiment used a set of query set of 30×19 samples. The experiment consists of many trials, in each one, the number of features involved in the classification is increased by one, starting by 5 features and ending by 35. The classification rate associated to the WTC and Zernike moments are mapped in Figure 4.(b). The Figure shows that the WTC have the best classification rate over all the number of features, with a maximum rate of 98% reached with 23 features. For Zernike moments the maximum rate of 94% is obtained with 28 features. Also we notice that with 11 WTC can guarantee a classification rate of 95% whereas a lower rate of 93% needs 16 Zernike moments.

Although there is an overall improvement of the classification performances as the number of features get increased, this improvement is not monotonous as there are some fluctuations that start at the 10th feature . Also after a certain number of features (25) the classification rate looks stagnating. We believe that this phenomena has its roots in the feature selection process, since the technique we used guarantee only a sub-optimal set of features.

5. Conclusion

This works described a framework and methodology to solve the problem of recognizing human body posture from a could of 3D data. A new 3D feature representation based on the coefficients of a wavelet transform was suggested. These fatures demonstrated very reasonable discriminative power compared to those of Zernike moments and geometric moments. The impact of the WTC performances was reflected in the experiments carried out to evaluate the classification rate of each category. The WTC had the highest classification rate whatever number of features is used. For some set of WTC features, the classification rate reached 98% whereas a larger number of Zernike moments is needed for the maximum rate of 94%. As improvement,

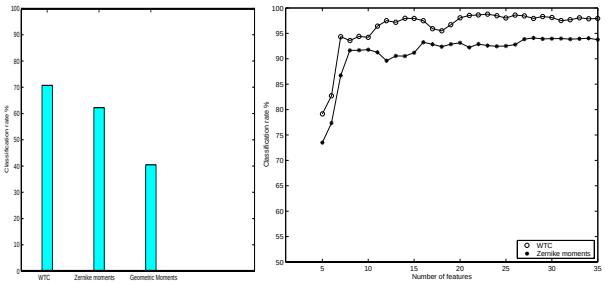

(a) (b)

Figure 4. Comparison of the classification rate of the three categories of features. (a) classification rate associated to the four geometric moments, 4 best WTC and 4 best Zernike moments. (b) Classification rate of the WTC and the Zernike moments mapped in function of the number of features.

the database of the training samples can be enriched by adding a variety of human body shapes coming from different scan sources. Naturally the number of model postures we considered is far from being exhaustive. Many others different postures can be added. This raises the question of what is the maximum number of different postures that could be successfully recognized. We believe that this is linked to what extent the recognition process could distinguish between two close postures and how to quantify the closeness of two postures. The adopted parametric description of the posture, mentioned in section 4.1, and describing a posture in terms of the rotation parameters associated to each body segment, can be used for that purpose. What remains is to determine the minimum changes in the values of the parameters that would produce a new distinguishable posture, This is what we are currently investigating.

References

[1] J. Starck, A.Hilton, J.Illingworth, "Human Shape Estimation in a Multi-Camera Studio". Proc. BMVC, pp.573-583, Manchester 2001.

[2] P. Jones, P.Li, K. Brook-Wavel, G. West, "Format of human body modelling from 3D body scanning", Int. Journal of Clothing Sciences, Vol.7, No.1, pp.7-16, 1995.

[3] R. Pargas, N. Staples, J.Davis, "Automatic measurement extraction for apparel for three-dimensional body scan", Journal of Optics and Laser engineering, Vol.28, PT2. , pp.157-172. 1996.

[4] L. Dekker, S.Khan, E.West, B.Buxton, "Models for understanding the 3D human body form". Proc. IEEE workshop on Model-Based 3D Image analysis, pp.65-74, Bombay, India, 1988.

[5] Civilian American and European Surface Anthropometry Resource, http://www.hec.afrl.af.mil/cardlab/caesar/

[6] M. Hu, "Visual pattern recognition by moment invariants", IRE Trans. On Information Theory, IT-8:pp. 179-187, 1962.

[7] M. Teague, Image Analysis via the general theory of moments, Journal of Optical Society of America. pp. 920-930, 70, 1980.

[8] C.H. Teh, R.T. Chin, "On Image Analysis by the methods of moments", IEEE Trans. PAMI Vol.10 pp. 496-513, 1988.

[9] F.A Sadjadi, E.L. Hall, "Three-Dimensional Moment Invariants", IEEE Trans. Pami, Vol.2 No. 2 March 1980.

[10] C. Lo, H. Don, "3-D Moment Forms: Their Construction and Application to Object Identification and Positioning", IEEE Trans. Pami Vol.11, No.10, October 1980.

[11] J. Morlet, A. Grossman. "Decomposition of Hardy Functions into Square Integrable Wavelets of Constant Shape" SIAM, J.Math.Anla, Vol.15, No.4, pp.723-736, July 1984.

[12] S. Mallat, "A Theory for Multiresolution Signal Decomposition: The Wavelet Representation", IEEE Trans. PAMI, Vol.11, No.7, pp.674-693, July 1989.

[13] I. Daubechies, "The Wavelet Transform, Time-Frequency Localization and Signal Analysis", IEEE Trans. Info.Theory, Vol.36, No.5, pp.961-1005, September 1990.

[14] Y. Meyer, "Wavelets: Algorithms & Applications", SIAM Ed. 1993

[15] N.M Ferrers, " An Elementary Treatise in Spherical Harmonics", MacMillan 1877.

[16] R. Redner, H.Walker, "Mixture densities, maximum likelihood and the EM algorithm", SIAM Review, Vol 26, No.2, 1984.

[17] K. Fukunaga, "Introduction to Statistical Pattern Recognition", 2nd Ed., Academic Press, New York, 1990.

[18] N. Canterakis, "Fast 3D Zernike Moments and Invariants", Tech. Report, 1997, Instistute of Informatic, University of Friburg,Germany.

[19] http://www.cyberware.com/

[20] "3D Anthropometric Measurement and Extraction System"

[21] "3D Animation of Human Body Model",